Phosphoproteome analysis of the human mitotic spindle

Marjaana Nousiainen*, Herman H. W. Silljé, Guido Sauer†, Erich A. Nigg, and Roman Körner‡

Department of Cell Biology, Max Planck Institute of Biochemistry, Am Klopferspitz 18, D-82152 Martinsried, Germany

Edited by Stephen J. Elledge, Harvard Medical School, Boston, MA, and approved January 8, 2006 (received for review August 15, 2005)

During cell division, the mitotic spindle segregates the sister chromatids into two nascent cells, such that each daughter cell inherits one complete set of chromosomes. Errors in spindle formation can result in both chromosome missegregation and cytokinesis defects and hence lead to genomic instability. To ensure the correct function of the spindle, the activity and localization of spindle associated proteins has to be tightly regulated in time and space. Reversible phosphorylation has been shown to be one of the key regulatory mechanisms for the organization of the mitotic spindle. The relatively low number of identified *in vivo* phosphorylation sites of spindle components, however, has hampered functional analysis of regulatory spindle networks. A more complete inventory of the phosphorylation sites of spindle-associated proteins would therefore constitute an important advance. Here, we describe the mass spectrometry-based identification of *in vivo* phosphorylation sites from purified human mitotic spindles. In total, 736 phosphorylation sites were identified, of which 312 could be attributed to known spindle proteins. Among these are phosphorylation sites that were previously shown to be important for the regulation of spindle-associated proteins. Importantly, this data set also comprises 279 novel phosphorylation sites of known spindle proteins for future functional studies. This inventory of spindle phosphorylation sites should thus make an important contribution to a better understanding of the molecular mechanisms that regulate the formation, function, and integrity of the mitotic spindle.

mass spectrometry | mitosis | molecular cell biology | phosphorylation | proteomics

At the transition from interphase to mitosis, the microtubule network undergoes a profound change that culminates in the formation of the spindle apparatus. The mitotic spindle then serves to segregate the chromosomes to opposite poles of the cell and to define the plane of cell division. A large number of proteins associate with this microtubule-based structure and regulate its dynamic formation and function (1, 2). Several spindle proteins, including XKCM1 and XMAP215 family members (3, 4), have been identified that either stabilize or destabilize microtubules by mediating the rapid changes between polymerization and depolymerization (5, 6). These proteins play an important role in spindle formation, as illustrated by the striking change in microtubule half-life from 5–10 min in interphase to less than 1 min in mitosis (7), which results in the short and unstable microtubules characteristic of mitosis (5, 6). Another important group of spindle proteins comprises motors of the kinesin and dynein families that are essential for mitotic progression (5, 6, 8, 9). They push the spindle poles away from each other during early mitosis and play crucial roles in capturing chromosomes and positioning them at the metaphase plate. Subsequently, motors also contribute to central spindle formation and cytokinesis. In addition, numerous structural proteins, including NuMA and Tpx2, are required for proper bipolar spindle formation (10, 11).

To ensure proper mitotic progression, the above-mentioned processes must be tightly controlled. Many spindle proteins have been shown to be phosphorylated in a cell-cycle-dependent manner (12), indicating that phosphorylation by protein kinases (and dephosphorylation by phosphatases) plays an important role in the regulation of spindle function. In support of this conclusion, a number of kinases, including Plk1 and Aurora-A and -B, show dynamic spindle localizations and are essential for proper mitotic progression. However, a detailed molecular understanding of the role of protein phosphorylation of spindle proteins has been restricted to a limited number of spindle proteins, largely because of technical difficulties in determining *in vivo* phosphorylation sites.

Protein phosphorylation has been conventionally analyzed by using radioactive labeling followed by two-dimensional gel electrophoresis, phosphopeptide mapping by thin-layer chromatography and electrophoresis, sequencing by Edman degradation, or site-directed mutagenesis. More recently, mass spectrometry has emerged as a key technology for mapping protein phosphorylation sites, owing to its high sensitivity and speed of analysis (13–17). Mapping of phosphorylation sites within complex protein mixtures, however, is still a difficult task because of the often low stoichiometry of phosphorylation and signal suppression by unphosphorylated peptides. Specific capture of phosphopeptides is possible by β-elimination of the phosphate group and subsequent introduction of an affinity tag (18–23), or by covalent capture and release (24). These two methods have been designed for enhanced specificity but involve complex chemistry and have not been widely used because of limited sensitivity. Alternatively, the simpler and more sensitive methods of phosphopeptide enrichment by strong cation exchange chromatography (25, 26) or immobilized metal ion chromatography (IMAC) (27, 28) have been used successfully for phosphoproteomics. The IMAC method is based on the affinity of di- or trivalent metal ions for phosphate groups, and despite some limitations, including nonspecific binding of peptides (29, 30) and the fact that not all phosphopeptides are retained equally efficiently on IMAC resins (26, 28, 31), this method has shown great promise for large-scale studies (29, 32, 33).

Recently, we have purified mitotic spindles from human HeLa S3 cells and identified a total of 795 proteins, including 151 previously known spindle-associated components (34). In this former study, we have also characterized the purity of the spindle preparations, using differential interference contrast microscopy, Western blot analyses with antibodies against known spindle and control proteins, tandem mass spectrometry (MS/MS), and cell biological validation experiments. Here, we extended this earlier study to the identification of phosphorylation sites in proteins of isolated mitotic spindles. Using mass spectrometry with and without prior IMAC-based enrichment of phosphopeptides, we have localized a total of 736 phosphorylation sites in 260 proteins, including 312 sites in 72 known

Conflict of interest statement: No conflicts declared.

This paper was submitted directly (Track II) to the PNAS office.

Abbreviations: ESI, electrospray ionization; IMAC, immobilized metal ion chromatography; MS/MS, tandem mass spectrometry; LC, liquid chromatography.

Data deposition: The data set reported in this paper has been deposited in the Proteomics Identification Database (PRIDE), www.ebi.ac.uk/pride (accession nos. 1628–1631).

*Present address: Laboratory of Applied Environmental Chemistry, University of Kuopio, P.O. Box 181, 50100 Mikkeli, Finland.

†Present address: Institute for Biochemistry, University of Göttingen, Humboldtallee 23, D-37073 Göttingen, Germany.

‡To whom correspondence should be addressed. E-mail: rkoerner@biochem.mpg.de.

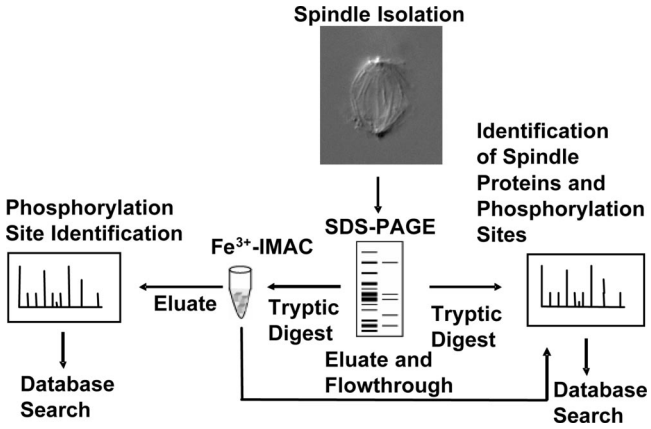

Fig. 1. Analytical strategy for the mapping of phosphorylation sites in spindle proteins. Mitotic spindles were isolated and proteins subsequently separated by SDS/PAGE. The gel was cut into 18 slices and trypsinized. The samples were batch-incubated with Fe^{3+}-IMAC resin, and eluted peptides were analyzed by nano-LC-ESI-MS/MS and nano-ESI-MS/MS. IMAC flow-through and samples not enriched by IMAC were analyzed by nano-LC-ESI-MS/MS.

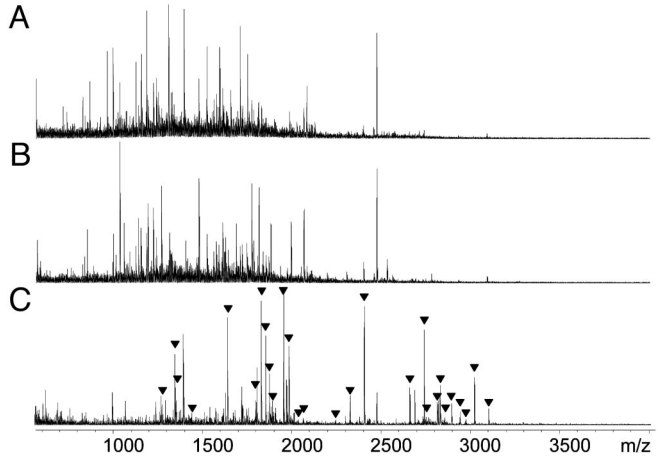

Fig. 2. Example of MALDI-TOF MS spectra of a phosphopeptide-containing sample before and after IMAC enrichment. (*A*) Before IMAC enrichments. (*B*) IMAC flow-through. (*C*) IMAC eluate. Peaks marked by filled triangles in *C* were identified as phosphopeptides in subsequent analyses.

spindle proteins. This data set was analyzed with regard to consensus sequences for selected kinases and phosphorylation-dependent protein–protein interaction motifs, providing a valuable resource for future studies on the regulation of the spindle apparatus.

Results

To identify phosphorylation sites in mitotic spindle proteins, an analytical strategy was developed based on our previously established spindle isolation protocol (Fig. 1) (34). Taxol-stabilized mitotic spindles (including kinetochores and centrosomes) were purified as described (34), and spindle proteins were separated on one-dimensional SDS/PAGE gradient gels. After Coomassie blue staining, each lane was cut into 18 pieces, covering different protein mass ranges. The proteins were then in-gel digested with trypsin, and extracted peptides were either directly identified by nano-liquid chromatography (LC)-electrospray ionization (ESI)-MS/MS or applied to phosphopeptide enrichment by Fe^{3+}-IMAC (see Fig. 1). After phosphopeptide isolation, the IMAC samples were analyzed by nano-LC-ESI-MS/MS and, without chromatographic separation, by nano-ESI-MS/MS (35). Peptides in the IMAC flow-throughs were identified by nano-LC-ESI-MS/MS (see Fig. 1).

Phosphopeptide Enrichment by IMAC and Identification of Phosphorylation Sites by MS/MS. For phosphopeptide enrichment, initial binding as well as washing steps were performed with the IMAC resins shaking in suspension instead of using an IMAC column. In this way, the resins could be washed more efficiently, and the background of unphosphorylated peptides was reduced. Methyl-esterification before IMAC has been proposed (29) as a means to reduce unspecific binding of acidic peptides. This method, however, was not used in this study because we observed reduced recovery of phosphopeptides after methyl-esterification. Using the improved washing protocol, we observed that 76% of all IMAC-eluted peptides were phosphorylated. This strong enrichment of phosphopeptides by Fe^{3+}-IMAC is illustrated in Fig. 2. The MALDI-TOF spectra of a sample (from a gel slice corresponding to a protein mass of ≈110 kDa) before IMAC (Fig. 2*a*) and the IMAC flow-through (Fig. 2*b*) are very similar whereas many phosphorylated peptides in the IMAC eluate (marked with filled triangles in Fig. 2*c* and confirmed by nano-ESI-MS/MS) were not detected in the original sample.

Peptides in the IMAC eluate were subjected to nano-LC-ESI-MS/MS and nano-ESI-MS/MS to allow the identification of the peptides and the localization of the phosphorylated residues within the peptide sequences. In total, 571 phosphorylation sites were detected by the nano-LC method, 149 phosphorylation sites were detected by nano-ESI-MS/MS without prior chromatographic separation, and 76 phosphorylation sites were detected by both methods (overlap).

Even though IMAC enriched efficiently for phosphorylated peptides, not all phosphopeptides bound equally well to the Fe^{3+}-loaded resins. Therefore, the flow-through fractions of the IMAC samples, and samples which were not enriched for phosphorylated peptides by IMAC, were also analyzed for the presence of phosphopeptides (see Fig. 1). In total, 644 phosphorylation sites were detected in IMAC eluates, 179 sites were found in samples that had not been enriched by IMAC, and 87 sites were detected by both approaches (overlap). In IMAC eluates, 31% of the phosphopeptides were multiply phosphorylated, whereas only 6% of the phosphopeptides in samples not subjected to IMAC had multiple phosphorylation sites. Thus, these IMAC samples were enriched in multiply phosphorylated peptides, which is in agreement with previous reports (29, 32) and can be explained by the stronger binding of multiply phosphorylated peptides to the Fe^{3+}-loaded resins.

Analysis of Identified Phosphorylation Sites. By using the described strategies, a total of 736 phosphorylation sites were identified in 260 proteins (see Table 4, which is published as supporting information on the PNAS web site). Among these, 312 phosphorylation sites were present in 72 known spindle proteins (see Table 1), confirming the relatively high purity of the spindle preparation. Importantly, 279 of the latter sites (89%) had, to the best of our knowledge, not previously been described. This data set provides information about many known spindle proteins, including major structural components (NuMA, Tpx2), kinesins (MKlp1 (KIF23), MKlp2 (Kif20A), Eg5 (KIF11), Kid (KIF22), KIF4A), and the chromosomal passenger complex (INCENP, Aurora-B, Survivin, and Borealin) (36). In addition to microtubule-associated proteins, the enriched spindle preparations also included phosphorylated proteins that localize to kinetochores (AF15q14, HEC, Mis6, Mis13, Mis14, Nuf2, Nup107, Nup133, Nup160, Spc24, and Zw10) and centrosomes (CAP350, Cep192, Cep215, Pericentrin 2, and PCM-1).

We have analyzed our data set for the frequencies of consensus recognition sites for the most important protein kinases involved in

Table 1. Phosphorylation sites of known spindle proteins

Protein	Phosphorylated residues
Abnormal spindle protein (Q8IZT6)	S14, S35, **S222**, S225, S263, S267, S270, S280, S283, S348, **S367, S370**, S392, S425, S463, T563, S605, T647, S1103, T3435
AF15q14 (Q9NR92)	S32, **S60**, S739, S741, S930, S1013, T1016, S1050, **S1747**
APC1 (Q9H1A4)	**S686, S688**
APC6 (Q13042)	**S560,** T581
APC8 (Q9UJX2)	**S582, T590**
Astrin (Q96R06)	S62, S66, T111, S135, S249, S334, S341, **S353, S362, S364, T377, T389,** S401, T937
Aurora-B (Q96GD4)	**Y12,** S7, **T232**
Borealin (Q96AM3)	**S219**
Casein kinase I (P48729)	**T321**
CENP-B (P07199)	S156, S165
CENP-C (Q03188)	T167, S170, S177, S316, S333, S538
CENP-E (Q02224)	**T422,** S454, S611, **S1211, T1267, S2601,** S2613, S2616
CENP-F (P49454)	S821, S1324, S1747, **S1750,** S1988, S2513, S2996, S3007, S3094, S3119, S3175, S3179
Cep192 (Q8TEP8)	S945, S949
Cep215 (Q96SN8)	S815, S1074, **S1238**
Cdc27 (P30260)	**S435, S438**
cdk1 (P06493)	**T161**
CAP350 (Q8WY20)	**S1818**
Citron Rho-interacting kinase (O14578)	**S440**
CLIP-170 (P30622)	**T182**
Condensin subunit 1 (Q15021)	S103, S585, S1330, **S1333, T1388**
Condensin subunit 2 (Q15003)	T49, S78, S81, S92, S96, S201, S335, T605
Condensin subunit 3 (Q9BPX3)	S390, S674
C20orf129 (Q9H4H8)	T513
DNA topoisomerase II, alpha isozyme (P11388)	**S1106, S1213,** S1247, **S1295, S1297,** S1351, S1354, S1387, S1393, **S1525**
DNA topoisomerase II, beta isozyme (Q02880)	S1471, **S1522, S1524**
Dynein light chain-A (Q9Y6G9)	**S207**
GEF-H1 (Q92974)	**S163,** S695
Haspin (Q8TF76)	T253
HSP 90-beta (P08238)	**S254**
HEC (O14777)	**S55, S62,** S76, S77
HURP (Q8NG58)	S662, S689, S777
Hyaluronan mediated motility receptor (O75330)	S20, **T703**
INCENP (Q5Y192)	Y73, S119, S142, S143, S148, S197, S199, T213, **S214, T219,** S230, T239, **S263,** S269, S275, S291, T292, **T294, S296, S306, S312,** S314, S421, T424, S481, **S828, S831, T832, S899, T892, S893, S894, S899**

Table 1. (continued)

Protein	Phosphorylated residues
KIAA1187 (Q9ULN3)	**S443, S517,** S521, **S525,** S806
KIF2 (O00139)	**T51, S113**
KIF4A (O95239)	**S507, S801, S810, S951, S1013,** S1017, S1038, S1126, T1161, T1181, S1186, **S1225**
KIF11/Eg5 (P52732)	**T927,** S932
Kif18a (Q8NI77)	**T706**
KIF20A/MKIp2 (O95235)	S49, **S244, S528,** S532, **S556, S867**
KIF22/Kid (Q14807)	S543, S581, S562
KIF23/MKIp1 (Q02241)	S160, **S682, S684, S807, S808**
LB1/TMAP (Q8IWV6)	S534, **T578,** T581, T596, **S601, T622**
MAD1 (Q9UNH0)	**S428**
MAP4 (P27816)	S825, T571, T521
MAP7 (Q14244)	S169, **S200, S209, S219, T231, T277,** S315, **S365,** S672, T673
MgcRacGAP (Q9P2W2)	**T161, S164, S170, S203, S214, T342, T580, T588, S590, S628**
Mis6/CENP-I (Q92674)	**S22**
Mis13 (Q9H410)	**S28,** S30
Mis14/DC8 (Q96IY1)	**T242**
Nuf2 (Q9BZD4)	**S247**
NuMA (Q14980)	**S169, S172, S200, S203, T211, S1262, S1721, S1724,** T1733, **S1757, S1769, S1772, T1776, S1830, S1833, S1834, S1837, S1862,** S1872, S1945, **T2000**
NuMa splice variant 1 (Q9BTE9)	S653, **S656,** S664
Nup98-Nup96 precursor (P52948)	**S888**
Nup107 (P57740)	**S4, S11, T46, T55, S58, T64**
Nup133 (Q8WUM0)	S27, T28, S45
Nup160 (Q12769)	**S1123**
NuSAP (Q9BXS6)	S135
Pericentrin 2 (O95613)	S1703
PCM-1 (Q15154)	**S65, S69, S992**
PP2A (Q14738)	S598
PRC1 (O43663)	**S195,** S592
RanBP2 (P49792)	T19, **S21, T2450, S2454**
RanGAP1 (P46060)	S428, **S442**
Septin 2 (Q15019)	**S218**
Survivin (O15392)	**T34**
Spc24 (Q8NBT2)	**T130**
Tpx2 (Q9ULW0)	T51, T72, **S121, S125,** T147, S186, **S293, T338,** S359, **T369, T374, S486, S542, S652, S654, S738**
Tubulin alpha (Q6PEY2)	**S48**
Similar to Tubulin alpha (gi|51476041)	S290
Tubulin beta (Q969E5)	**T290**
Zw10 (O43264)	**T437**

The underlined sites were previously published, and the sites in bold are conserved. Accession numbers of phosphoproteins are given in parentheses.

mitosis (Cdk1, Plk1, and Aurora kinases) (Table 2). As expected, the consensus site for Cdk1 (or other proline-directed kinases) was most frequent among the observed phosphorylation sites, followed by the consensus sites for Plk1. In addition, we asked whether consensus sites for the phosphopeptide-binding domain of Plk1, the so-called polo box domain (PBD) (37), were present among the identified phosphorylated peptides. As shown in Table 2, a considerable number of PBD-binding sites matching the consensus S-pS/pT were indeed found in spindle proteins. No significant differences were observed between known spindle proteins and other proteins regarding the frequency distribution of the sites analyzed (see Fig. 3, which is published as supporting information on the PNAS web site).

In addition, we analyzed the spindle protein data set using the SCANSITE program (38), which can be used to predict phosphorylation sites for selected kinases as well as certain phosphorylation-dependent binding motifs. Table 3 indicates the number of

Table 2. Manually scanned motifs

	Motif	Hits
Cdk1	pS/pT-P	166
Polo-like kinase 1 (Plk1)	D/E-X-pS/pT	62
Aurora-A, Aurora-B	R/K-R/K-X-pS/pT	9
Polo-box binding domain	S-pS/pT	33

matches between experimentally detected phosphorylation sites within known spindle proteins and SCANSITE-predicted phosphorylation sites at high and low stringency levels, respectively (38). A complete list of the matching phosphopeptides is presented as Table 5, which is published as supporting information on the PNAS web site. Again, sites phosphorylated by proline-directed kinases were most commonly predicted. In addition, several experimentally determined sites were found to conform to predictions for calcium/calmodulin-dependent kinase 2, followed by the acidophilic kinase group comprising casein kinase 1 and 2 as well as glycogen synthase kinase 3 (GSK3). Potential binding sites for 14-3-3 proteins could only be detected upon running SCANSITE searches in low stringency mode.

Evolutionary Conservation of Phosphorylation Sites. Functionally important phosphorylation sites are often evolutionarily conserved among related species. Therefore, multiple sequence alignments for the available orthologs from mouse, chicken, *Xenopus laevis*, and zebrafish or pufferfish were made by using CLUSTALW (www.ebi.ac.uk/clustalw). Forty-six percent of all experimentally detected spindle protein phosphorylation sites were conserved in at least three (human and two other) of the selected species, indicating that many of the detected phosphorylation sites may be functionally relevant (Table 1, sites in bold). Evolutionary conservation constitutes a useful criterion for selecting particular phosphorylation sites for functional analysis, but it is clear that direct cell biological validation experiments will be required to demonstrate the functional significance of any particular phosphorylation sites and to explore its function in the regulation of the mitotic spindle apparatus.

Discussion

Numerous spindle proteins have been shown to be phosphorylated in a cell cycle-dependent manner, indicating that phosphorylation by kinases and dephosphorylation by phosphatases play an important role in the function and regulation of the mitotic spindle (12). Our aim, therefore, was to reveal specific phosphorylation sites in spindle components by a phosphoproteome approach. Using complementary strategies, including phosphopeptide enrichment by IMAC, we identified >700 phosphorylation sites by MS/MS, of which >300 were found in known spindle proteins.

The phosphorylation sites within IMAC-enriched peptides were mapped by using both nano-LC-ESI-MS/MS and nano-ESI-MS/MS. In comparison with nano-LC-ESI-MS/MS, nano-ESI-MS/MS allows for longer data acquisition times for phosphopeptides of low abundance, which is due to its ≈10 times lower flow rate and the lack of chromatographic separation. This lack of chromatographic separation, however, leads also to suppression effects in complex peptides mixtures, and nano-ESI-MS/MS is therefore mostly used for samples of low and medium complexity. Because almost four times more phosphopeptides were detected by using the nano-LC approach (see *Results*), we conclude that our samples were too complex for the analysis of unseparated phosphopeptide mixtures. Interestingly, however, 73 phosphorylation sites of the IMAC eluates were only detected without prior separation by nano-LC. This result demonstrates that the data sets are complementary and that phosphorylation site mapping of complex samples by alternative strategies can lead to an increased total number of detected phosphorylation sites.

In addition to the identification of numerous novel phosphorylation sites, we could confirm previously described *in vivo* and *in vitro* phosphorylation sites. For example, the phosphorylation site Thr-927 in Eg5 (KIF11) has previously been shown to regulate spindle association of Eg5 (KIF11) (39), and phosphorylation of Thr-34 in survivin by Cdk1 has been related to the regulation of apoptosis during M phase (40). The previously described phosphorylation sites further included the activation loop sites of Aurora-B (Thr-232) (41) and Cdk1 (T161) (42) as well as the major Plk1 phosphorylation site (and PBD-binding site) in MKlp2 (KIF20A) (Ser-528) (43). We could also validate *in vivo* phosphorylation of sites that had previously been observed only *in vitro*. For example, *Xenopus* Tpx2 had been reported to be phosphorylated by Aurora-A *in vitro* on Ser-90 and Ser-94 (44), and we have now identified phosphorylation of the corresponding sites in endogenous human Tpx2 (Ser-121 and Ser-125). The functions of these phosphorylations are not yet known, and it should be noted that although these sites are conserved between human, mouse, and *Xenopus*, they are not present in chicken Tpx2. Similarly, we have identified endogenous phosphorylation of Ser-911 and Ser-912 in MKlp1 (KIF23), two conserved residues that could be phosphorylated by Plk1 *in vitro* (45).

The most extensively phosphorylated spindle protein identified in our screen was INCENP with 33 phosphorylation sites. Three of these sites (T892, S893, and S894), located in the C-terminal IN-box, were previously shown to be important for Aurora-B kinase activation (46), but the functions of the other sites are so far unknown. In yeast, dephosphorylation of INCENP (Sli15) by Cdc14 is important for its relocalization from the kinetochore to the spindle (47). Considering that human INCENP is also a substrate of Cdc14, at least *in vitro* (48), it is attractive to speculate that reversible phosphorylation of some of the identified sites may contribute to regulate the localization of INCENP. In addition to serine/threonine phosphorylation, both INCENP and its interacting kinase Aurora-B were found to be phosphorylated on tyrosine residues. Although the tyrosine residue in INCENP (Tyr-73) is not conserved in other vertebrates, the Aurora-B residue (Y12) is clearly conserved in mouse and *Xenopus*. This finding suggests that the chromosomal passenger complex could be regulated by a tyrosine or dual-specificity kinase.

Most phosphorylation sites identified here were followed by proline residues, indicating that Cdk1 is probably the major

Table 3. SCANSITE prediction at high stringency (0.2%) and low stringency (5%) for kinase phosphorylation and binding motifs from the data set of spindle protein phosphorylation sites

SCANSITE predictions	Hits, high stringency	Hits, low stringency
Basophilic serine/threonine kinase group		
Calmodulin-dependent kinase 2	0	11
DNA damage kinase group		
DNA PK	0	10
ATM	2	20
Acidophilic serine/threonine kinase group		
Casein kinase 2	4	20
Casein kinase 1	0	7
GSK3	3	19
Proline-dependent serine/threonine kinase group		
p38	3	36
Erk1	5	44
Cdk1	4	85
Phosphoserine/threonine binding group		
14-3-3 mode 1	0	9

kinase phosphorylating spindle proteins. In addition, some of these sites could be targeted by other proline-directed kinases, notably members of the MAP kinase family (see Tables 2 and 3). An important role in spindle formation and function has also been attributed to Plk1 and Aurora kinases. In support of this view, we also found a substantial number of peptides bearing phosphorylation consensus sites for these kinases. Moreover, many peptides were identified with phosphorylations within consensus Plk1 PBD-docking sites (37), suggesting that Plk1 might interact with, and potentially phosphorylate, a substantial number of spindle proteins. The actual number of PBD-docking proteins may be even higher, considering that an alternative Plk1-docking site has been identified by Neef *et al.* (43).

Current bioinformatic algorithms are largely based on *in vitro* analyses using recombinant kinases and synthetic phosphopeptides libraries. To enhance the power of such prediction tools, it will be important to incorporate additional parameters, including protein structure data, information about the subcellular localization of substrates and kinases, and expressions patterns. In this context, we anticipate that the availability of experimental data sets derived from *in vivo* phosphorylation analyses will assist the development and fine-tuning of prediction algorithms.

Finally, we trust that the present data set constitutes a valuable starting point for future functional studies on spindle structure and dynamics, and thus may contribute to the identification of novel regulatory mechanisms controlling spindle function. Given that regulatory protein phosphorylation is highly dynamic, an extension of our present study to the analysis of the variations in spindle protein phosphorylation during mitotic progression would allow further insight into the temporal regulation of the mitotic spindle. Such analyses may also reveal to what extent reversible phosphorylation triggers the relocalization of many spindle proteins during cell division, and thus might link temporal protein phosphorylation to the spatial organization of spindle assembly.

Experimental Procedures

Materials. Unless otherwise stated, chemicals were purchased from Sigma or Fluka. NuPAGE Bis-Tris gels (1.0 mm thick, nine lanes per gel) were purchased from Invitrogen. Sequencing-grade modified trypsin was from Promega. POROS 20 MC and oligo R3 chromatographic materials were purchased from Applied Biosystems, $FeCl_3$ was purchased from BDH, and 2,5-dihydroxybenzoic acid matrix was purchased from Bruker Daltonics. Nanoscale IMAC columns were packed in GELoader tips (Eppendorf).

Cell Culture and Mitotic Spindle Isolation. HeLa S3 cells were maintained in DMEM containing 10% FCS, 50 units/ml penicillin, and 50 μg/ml streptomycin. Cells were grown at 37°C in a humidified incubator with a 5% CO_2 atmosphere. Taxol-stabilized mitotic spindles (including kinetochores and centrosomes) were purified as described in ref. 34, except that okadaic acid (100 nM) was added to all buffers to prevent dephosphorylation by PP2A- and PP1-type protein phosphatases. In short, HeLa S3 cells were synchronized in mitosis by using a sequential aphidicolin block/release, nocodazole block protocol. After shake-off and release of mitotic cells, taxol was added to stabilize microtubules when most cells had reached a metaphase stage. After lysis, the cells were treated with DNAses to remove chromosomes and with latrunculin B to depolymerize the actin cytoskeleton. Finally, intermediate filaments were depolymerized in low-ionic-strength buffer, and the mitotic spindles were collected by centrifugation.

Gel Electrophoresis and In-Gel Digestion. Two hundred micrograms of acetone-precipitated spindle proteins were dissolved in 19 μl of lithium dodecyl sulfate (LDS) sample buffer and 2 μl of 0.5 M DTT and heated for 5 min at 95°C. The mixture was divided into five lanes of a NuPAGE Bis-Tris gradient gel and run for 50 min using a 200-V/110-mA program. The gel was stained with a 1:1 mixture of 0.2% Coomassie blue in MeOH and 20% acetic acid, and destained first with a mixture of 7% acetic acid and 30% EtOH, and subsequently with 10% acetic acid. Complete lanes were cut into 18 pieces each, and the corresponding pieces from the three lanes were combined. The protein bands were in-gel digested by trypsin (49), and after 16 h the digestions were stopped by addition of formic acid to a final concentration of 1%. The peptides were extracted from the gel by using 5% formic acid and 100% acetonitrile and dried by lyophilization.

Immobilized Metal-Ion-Affinity Chromatography and Desalting. Five milligrams of POROS 20 MS resin was placed in a 1.5-ml plastic tube and washed subsequently with 1-ml volumes of H_2O, 50 mM EDTA in 1 M $NaCl_2$, H_2O, 0.6% acetic acid, three times with 0.1 M $FeCl_3$ in 0.6% acetic acid, H_2O, 100 mM NaCl, 0.6% acetic acid, a 3:1 mixture of 0.6% acetic acid and acetonitrile, and two times with 0.6% acetic acid.

After each of the washing steps, the tube containing the resin was centrifuged for 30 sec, and the washing buffers were carefully removed with a pipette from the settled resins. Three microliters of the settled resin was mixed with the tryptic peptide mixture in 80 μl of 0.6% acetic acid for 15 min in a shaker. The resin was centrifuged, and the supernatant was collected for subsequent analysis of unbound peptides. After a 5-min washing step in a shaker with 200 μl of 0.6% acetic acid, the supernatant was collected. The resin was washed further with 200 μl of a 3:1 mixture of 0.6% acetic acid and acetonitrile for 5 min in a shaker before the slurry was loaded into a GELoader tip, which had been narrowed at the outlet. The flow-through was collected and the column washed with 40 μl of a 3:1 mixture of 0.6% acetic acid and acetonitrile and two times with 40 μl of 0.6% acetic acid to remove the remaining unbound peptides from the column. The bound peptides were finally eluted with 2× 10 μl of 0.6% ammonia and instantly acidified with 20 μl of 10% formic acid.

Desalting of samples for mass spectrometric analysis was performed by using homemade miniaturized reversed-phase columns of oligo R3 packing material (50). The column was washed with 0.1% formic acid and eluted with a 1:1 mixture of MeOH/water containing 2% formic acid.

Mass Spectrometry. MALDI-TOF mass spectra were acquired on a Reflex III instrument (Bruker Daltonics) in both positive and negative reflector modes. 2,5-Dihydroxybenzoic acid (Bruker Daltonics) was used as a matrix for phosphopeptide samples on an AnchorChip 384-well target plate (Bruker Daltonics).

For peptide sequencing by MS/MS, samples were dissolved in water/methanol (1:1, vol/vol) containing 2% formic acid, filled into nanospray needles (Proxeon, Odense, Denmark), and analyzed by using nano-ESI on a quadrupole time-of-flight (Q-TOF) mass spectrometer (Q-TOF Ultima; Waters).

For nano-LC-MS/MS, samples were eluted from a pulled fused silica capillary with an internal diameter of 75 μm and a tip of 8 μm (New Objective, Woburn, MA) packed to a length of 13 cm with 3-μm reversed-phase material ReproSil-Pur C18-AQ (Maisch, Ammerbuch, Germany) directly into the Q-TOF mass spectrometer. Peptides were separated by a stepwise 90-min gradient of 0–100% between buffer A (2% acetonitrile/0.5% formic acid) and buffer B (80% acetonitrile/0.5% formic acid) from a CapLC HPLC system (Waters) at a flow rate of 170 nl/min. Throughout the analysis, 1.5-sec MS acquisitions were followed by 5.4-sec MS/MS experiments in information-dependent acquisition mode.

Protein Identification and Data Processing. The data obtained with ESI-MS/MS were processed by using MASSLYNX software (Waters) or Mascot Distiller (Matrix Science, London) for the submission of data to the protein and peptide search software

MASCOT (Matrix Science). Peak lists were searched against the Mass Spectrometry protein sequence DataBase (MSDB) (http://csc-fserve.hh.med.ic.ac.uk/msdb.html) or the International Protein Index database (www.ebi.ac.uk/IPI/IPIhelp.html). Searches were performed with precursor and fragment ion tolerances of 0.15 Da. Proteins identified by two or more peptides with a combined peptide score of >50 or by one single peptide with a score of >60 were considered significant, whereas all lower-scoring proteins were either included or discarded after inspection of individual spectra (using the criteria stated below). Phosphopeptides identified with a peptide score of ≥10 were considered to be potentially significant. For all of these peptides, MASCOT search hits and exact phosphorylation sites were confirmed or rejected by visually interpreting MS/MS ion spectra, resulting in an average MASCOT score of 46 for accepted phosphorylation sites. Criteria for the visual interpretation of MS/MS spectra included, primarily, that the majority of the m/z peaks in the spectra could be assigned to y- and b-type ions or to the loss of phosphoric acid from such fragments. Additional criteria were the presence of intense proline-directed fragment ions, the correct molecular mass of the corresponding protein as estimated from the region excised from the gel, and the detection of other peptides originating from the same protein in the same sample or the IMAC flow-through. Furthermore, phosphopeptides were only included in our data set if the presence of phosphospecific fragment ions allowed the unambiguous localization of the phosphorylated residue within the peptide sequence. Unprocessed mass spectrometry data files (in Waters .raw format) and peaklists can be downloaded from our web site (www.biochem.mpg.de/spindle_MS_spectra/) for further data validation.

We found confirmation of phosphorylation sites by visual interpretation of spectra essential because the MASCOT-search results often suggested incorrect sites for phosphorylation (especially for peptides with potential phosphorylation sites next to each other), although the peptide identification was correct.

Bioinformatics. Orthologs of spindle proteins were found by BLAST search (www.ncbi.nlm.nih.gov/blast) using full-length protein sequences of human proteins against nonredundant databases. CLUSTALW (www.ebi.ac.uk/clustalw) was used for protein-sequence alignments, and the SCANSITE program (http://scansite.mit.edu) was used for an analysis of consensus sites for selected kinases and protein-docking motifs (38).

We thank Albert Ries for cell culture work and isolation of mitotic spindles, as well as for excellent technical assistance. We are also very grateful for the help of Dr. Henning Hermjakob and Philip Jones from the European Bioinformatic Institute for the submission of our data set to the Proteomics Identification Database (PRIDE). This collaboration with the European Bioinformatic Institute was established within the Experimental Network for Functional INtegration European Network of Excellence, which is funded by the European Commission within its FP6 Programme, under the thematic area "Life sciences, genomics and biotechnology for health," Contract LSHG-CT-2005-518254. This work was supported by the Max Planck Society, a Marie Curie Individual Fellowship (to M.N.), and the Fonds der Chemischen Industrie (to E.A.N.).

1. Downing, K. H. & Nogales, E. (1998) *Curr. Opin. Struct. Biol.* **8,** 785–791.
2. Nogales, E. (2000) *Annu. Rev. Biochem.* **69,** 277–302.
3. Desai, A., Verma, S., Mitchison, T. J. & Walczak, C. E. (1999) *Cell* **96,** 69–78.
4. Kinoshita, K., Habermann, B. & Hyman, A. A. (2002) *Trends Cell Biol.* **12,** 267–273.
5. Desai, A. & Mitchison, T. J. (1997) *Annu. Rev. Cell Dev. Biol.* **13,** 83–117.
6. Howard, J. & Hyman, A. A. (2003) *Nature* **422,** 753–758.
7. Compton, D. A. (2000) *Annu. Rev. Biochem.* **69,** 95–114.
8. Sharp, D. J., Rogers, G. C. & Scholey, J. M. (2000) *Nature* **407,** 41–47.
9. Wittmann, T., Hyman, A. & Desai, A. (2001) *Nat. Cell Biol.* **3,** E28–E34.
10. Cleveland, D. W. (1995) *Trends Cell Biol.* **5,** 60–64.
11. Gruss, O. J., Wittmann, M., Yokoyama, H., Pepperkok, R., Kufer, T., Sillje, H., Karsenti, E., Mattaj, I. W. & Vernos, I. (2002) *Nat. Cell Biol.* **4,** 871–879.
12. Cassimeris, L. & Spittle, C. (2001) *Int. Rev. Cytol.* **210,** 163–226.
13. Kalume, D. E., Molina, H. & Pandey, A. (2003) *Curr. Opin. Chem. Biol.* **7,** 64–69.
14. McLachlin, D. T. & Chait, B. T. (2001) *Curr. Opin. Chem. Biol.* **5,** 591–602.
15. Mann, M. & Jensen, O. N. (2003) *Nat. Biotechnol.* **21,** 255–261.
16. Mann, M., Ong, S. E., Gronborg, M., Steen, H., Jensen, O. N. & Pandey, A. (2002) *Trends Biotechnol.* **20,** 261–268.
17. Sickmann, A., Mreyen, M. & Meyer, H. E. (2003) *Adv. Biochem. Eng. Biotechnol.* **83,** 141–176.
18. Adamczyk, M., Gebler, J. C. & Wu, J. (2001) *Rapid Commun. Mass Spectrom.* **15,** 1481–1488.
19. Goshe, M. B., Conrads, T. P., Panisko, E. A., Angell, N. H., Veenstra, T. D. & Smith, R. D. (2001) *Anal. Chem.* **73,** 2578–2586.
20. McLachlin, D. T. & Chait, B. T. (2003) *Anal. Chem.* **75,** 6826–6836.
21. Oda, Y., Nagasu, T. & Chait, B. T. (2001) *Nat. Biotechnol.* **19,** 379–382.
22. Qian, W. J., Goshe, M. B., Camp, D. G., Yu, L. R., Tang, K. & Smith, R. D. (2003) *Anal. Chem.* **75,** 5441–5450.
23. Thaler, F., Valsasina, B., Baldi, R., Xie, J., Stewart, A., Isacchi, A., Kalisz, H. M. & Rusconi, L. (2003) *Anal. Bioanal. Chem.* **376,** 366–373.
24. Zhou, H., Watts, J. D. & Aebersold, R. (2001) *Nat. Biotechnol.* **19,** 375–378.
25. Ballif, B. A., Villen, J., Beausoleil, S. A., Schwartz, D. & Gygi, S. P. (2004) *Mol. Cell. Proteomics* **3,** 1093–1101.
26. Beausoleil, S. A., Jedrychowski, M., Schwartz, D., Elias, J. E., Villen, J., Li, J., Cohn, M. A., Cantley, L. C. & Gygi, S. P. (2004) *Proc. Natl. Acad. Sci. USA* **101,** 12130–12135.
27. Andersson, L. & Porath, J. (1986) *Anal. Biochem.* **154,** 250–254.
28. Posewitz, M. C. & Tempst, P. (1999) *Anal. Chem.* **71,** 2883–2892.
29. Ficarro, S. B., McCleland, M. L., Stukenberg, P. T., Burke, D. J., Ross, M. M., Shabanowitz, J., Hunt, D. F. & White, F. M. (2002) *Nat. Biotechnol.* **20,** 301–305.
30. Muszynska, G., Dobrowolska, G., Medin, A., Ekman, P. & Porath, J. O. (1992) *J. Chromatogr.* **604,** 19–28.
31. Xhou, W., Merrick, B. A., Khaledi, M. G. & Tomer, K. B. (2000) *J. Am. Soc. Mass Spectrom.* **11,** 273–282.
32. Nuhse, T. S., Stensballe, A., Jensen, O. N. & Peck, S. C. (2003) *Mol. Cell. Proteomics* **2,** 1234–1243.
33. Shu, H., Chen, S., Bi, Q., Mumby, M. & Brekken, D. L. (2004) *Mol. Cell. Proteomics* **3,** 279–286.
34. Sauer, G., Körner, R., Hanisch, A., Ries, A., Nigg, E. A. & Sillje, H. W. (2005) *Mol. Cell. Proteomics* **4,** 35–43.
35. Wilm, M. & Mann, M. (1996) *Anal. Chem.* **68,** 1–8.
36. Vagnarelli, P. & Earnshaw, W. C. (2004) *Chromosoma* **113,** 211–222.
37. Elia, A. E., Cantley, L. C. & Yaffe, M. B. (2003) *Science* **299,** 1228–1231.
38. Obenauer, J. C., Cantley, L. C. & Yaffe, M. B. (2003) *Nucleic Acids Res.* **31,** 3635–3641.
39. Blangy, A., Lane, H. A., d'Herin, P., Harper, M., Kress, M. & Nigg, E. A. (1995) *Cell* **83,** 1159–1169.
40. O'Connor, D. S., Grossman, D., Plescia, J., Li, F., Zhang, H., Villa, A., Tognin, S., Marchisio, P. C. & Altieri, D. C. (2000) *Proc. Natl. Acad. Sci. USA* **97,** 13103–13107.
41. Yasui, Y., Urano, T., Kawajiri, A., Nagata, K., Tatsuka, M., Saya, H., Furukawa, K., Takahashi, T., Izawa, I. & Inagaki, M. (2004) *J. Biol. Chem.* **279,** 12997–13003.
42. Atherton-Fessler, S., Parker, L. L., Geahlen, R. L. & Piwnica-Worms, H. (1993) *Mol. Cell. Biol.* **13,** 1675–1685.
43. Neef, R., Preisinger, C., Sutcliffe, J., Kopajtich, R., Nigg, E. A., Mayer, T. U. & Barr, F. A. (2003) *J. Cell Biol.* **162,** 863–875.
44. Eyers, P. A. & Maller, J. L. (2004) *J. Biol. Chem.* **279,** 9008–9015.
45. Liu, X., Zhou, T., Kuriyama, R. & Erikson, R. L. (2004) *J. Cell Sci.* **117,** 3233–3246.
46. Honda, R., Körner, R. & Nigg, E. A. (2003) *Mol. Biol. Cell* **14,** 3325–3341.
47. Pereira, G. & Schiebel, E. (2003) *Science* **302,** 2120–2124.
48. Grüneberg, U., Neef, R., Honda, R., Nigg, E. A. & Barr, F. A. (2004) *J. Cell Biol.* **166,** 167–172.
49. Shevchenko, A., Wilm, M., Vorm, O. & Mann, M. (1996) *Anal. Chem.* **68,** 850–858.
50. Gobom, J., Nordhoff, E., Mirgorodskaya, E., Ekman, R. & Roepstorff, P. (1999) *J. Mass Spectrom.* **34,** 105–116.